$ReSe_2$ as a saturable absorber in a Tm-doped yttrium lithium fluoride (Tm:YLF) pulse laser

Chun Li (李 春)[1,2,3], Yuxin Leng (冷雨欣)[2,*], and Jinjin Huo (霍金金)[4]

[1]*School of Physics Science and Engineering, Tongji University, Shanghai 200092, China*
[2]*State Key Laboratory of High Field Laser Physics, Shanghai Institute of Optics and Fine Mechanics, Chinese Academy of Sciences, Shanghai 201800, China*
[3]*University of Chinese Academy of Sciences, Beijing 100049, China*
[4]*Jingjiang Photoelectric Technology Co., Ltd., Jinan 250000, China*
**Corresponding author: lengyuxin@mail.siom.ac.cn*

Received September 4, 2018; accepted November 23, 2018; posted online December 27, 2018

This study investigates the applicability of a few-layer structure $ReSe_2$ as a saturable absorber (SA) for demonstrating a passively Q-switched pulse laser. The $ReSe_2$ SA had a modulation depth of 6.86%. The Q-switched experiment was successful in delivering a maximum average output power of 180 mW at the wavelength of 1906.5 nm. The optimal pulse train had a pulse width of 1.61 μs and a repetition rate of 28.78 kHz. The experiment results verify that the few-layer structure $ReSe_2$ could behave as an excellent SA at all-solid-state lasers, increasing the selection of SAs at near 2 μm lasers.

OCIS codes: 140.3580, 140.3540, 160.4330.
doi: 10.3788/COL201917.011402.

All-solid-state passively Q-switched lasers have wide applications in a variety of fields because of their high peak power, short pulse width, simple structure, high efficiency, and low cost. A saturable absorber (SA) is a significant component of Q-switched lasers, and its development directly affects the improvement of pulse laser performance. After decades of development, traditional SAs, including organic dyes, semiconductor saturable absorption mirrors (SESAMs) and carbon nanotubes have been widely used for demonstrating pulse lasers[1–3]. However, organic dyes are toxic. SESAMs have the weakness of high-cost and narrow absorption bands[4–6]. Carbon nanotubes exhibit the disadvantages of strong non-saturable losses and limits by diameter/chirality control for realizing a broadband[5,6]. Therefore, researchers are constantly exploring ideal SA materials with characteristics of safety, low cost, simple preparation method, wide absorption band, high damage threshold, fast recovery time, and so on.

Until 2009, Bao *et al.* and Zhang *et al.* employed an atomic layer graphene as an SA to achieve a pulse operation with fiber lasers[7,8]. These experiments proved that atomic layer graphene could be applied as an SA to achieve pulse lasers and had triggered the investigation of two-dimensional (2D) materials in the field of lasers. As SA materials, graphene has ultrafast recovery time and low saturation intensity[6–10]. However, the low absorption efficiency restrains its progress due to the absence of band gap. Nowadays, transition metal dichalcogenides (TMDs) are another rapidly developed 2D material, and they own a band gap structure, which makes them more suitable for optoelectronic applications than graphene with zero band gap. 2D TMDs have admirable optical, electrical, thermal, and mechanical properties, such as strong optical absorption and relatively high charge carrier mobility[11,12]. In 2013, Wang *et al.* reported the nonlinear saturable absorption property of 2D MoS_2 (one type of TMDs) nanosheets, which confirmed its competence to act as an SA[13]. Then, in 2014, using MoS_2 as an SA, Zhang *et al.* demonstrated the ultrafast pulse generation, Liu *et al.* and Khazaeizhad *et al.* obtained the femtosecond pulse output in erbium-doped fiber lasers, and Xu *et al.* first, to the best of our knowledge, studied the passively Q-switched properties in an all-solid-state laser[14–17].

Following MoS_2 SA, $MoSe_2$, WS_2, and WSe_2 have also been concentrated on in studies, and become the representative of 2D TMDs[18–23]. They have significantly promoted the applications of 2D TMDs material as SAs. However, the MoS_2 class has signally variable optoelectrical characteristics as soon as the number of layers changes[24]. For the 2D MoS_2 class, the number of layers needs strict control, which brings great difficultly to the preparation[24]. Now, the uniform single-layer materials are still difficult to efficiently obtain in large numbers.

Recently, rhenium diselenide ($ReSe_2$) materials, whose characteristics are not sensitive to the number of layers, have attracted a lot of interest. $ReSe_2$ is a kind of semiconductor TMDs with the chemical formula MX_2, where M is transition metal ions, and X represents chalcogen ions. Layered TMDs are a sandwiched structure, where the upper and lower layers of X atoms sandwich a layer of M atoms in between[11,24]. They are combined by weak van der Waals interaction between layers and strong in-plane covalent bonding. So, bulk $ReSe_2$ could be exfoliated into 2D structures. More importantly, unlike MoS_2-class TMDs, bulk $ReSe_2$ owns a distorted 1T structure with triclinic symmetry[25–27]. The distorted 1T structure renders the weaker interlayer coupling action, which makes $ReSe_2$ behave as electronically and vibrationally

 © 2019 Chinese Optics Letters

decoupled monolayers[28,29]. Therefore, their characteristics are not sensitive to the number of layers. This greatly reduces the design and fabrication requirements for obtaining few-layer materials, which is beneficial to its applicability to 2D optical detectors, hydrogen evolution reaction, and field effect transistors[30–33]. Focusing on its saturable absorption characteristics, the report confirms $ReSe_2$ as an SA in a 1.55 μm fiber laser[34]. However, as a kind of broadband material, the saturable absorption characteristics of $ReSe_2$ in a near 2 μm waveband have not been studied.

In this contribution, we demonstrated the saturable absorption ability of $ReSe_2$ at the near 2 μm solid-state laser. A Tm-doped yttrium lithium fluoride (Tm:YLF) crystal was chosen as the laser material to acquire the near 2 μm laser, and the $ReSe_2$ was employed as an SA. Its modulation depth and saturation intensity were 6.86% and 23.37 kW/cm^2. The pulse laser obtained a maximum average output power of 180 mW, pulse duration of 1.61 μs, repetition rate of 28.78 kHz, pulse energy of 6.25 μJ, and peak power of 3.88 W. The experiment proved that $ReSe_2$ had saturable absorption characteristics and was confirmed to work as an SA in a near 2 μm solid-state laser.

Figure 1 shows the Raman spectrum of $ReSe_2$ powder within the frequency range from 100 to 300 cm^{-1}, which was measured by a Raman spectrometer (LabRAM HR Evolution, Horiba). Many peaks were observed due to the complex lattice vibration of $ReSe_2$, and obvious peaks including E_g and A_g modes were presented. In our experiment, $ReSe_2$ powder was added into alcohol for preparing $ReSe_2$ dispersion solution. The mass of $ReSe_2$ powder was 0.5 mg, and the volume of alcohol was 200 mL with a concentration of 15%. The dispersion solution was ultrasonicated for 48 h and then was quietly placed for 24 h. The supernatant was extracted to test the material morphology. A transmission electron microscope (TEM) scan image is exhibited in Fig. 2. With the optical resolution 50 nm of the TEM (JEM-2100), the TEM scan image

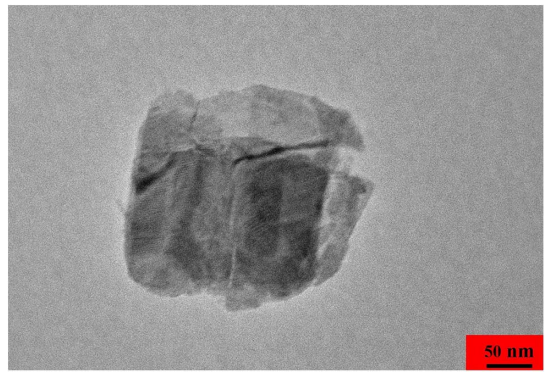

Fig. 2. TEM scan image of $ReSe_2$ in solution.

shows a few-layer structure of the sample. So, using a simple and efficient ultrasonic stripping technology, $ReSe_2$ with a few-layer structure was obtained. To acquire the $ReSe_2$ SA, the supernatant was spread on sapphire, which was placed in a drying cabinet for 24 h.

In order to verify whether $ReSe_2$ could act as an SA, a power-dependent transmission experiment was carried out to characterize the nonlinear optical response. The laser source was a home-made mode-locked Tm-doped fiber laser, whose pulse width and repetition rate were 26 ps and 12.36 MHz, respectively. The maximum output power was 76 mW at the central wavelength of 1910.3 nm. The Tm-doped fiber laser was injected into the $ReSe_2$ sample with spot diameter of 220 μm. The input power and the corresponding transmittance were recorded. Experimental data was fitted by

$$T(I) = 1 - T_{ns} - \Delta T \times \exp(-I/I_{sat}), \tag{1}$$

where T is the transmission, T_{ns} is the non-saturable absorbance, ΔT is the modulation depth, I is the input intensity of the laser, and I_{sat} is the saturation intensity[35,36]. Figure 3 shows the experimental data and the fitted curve. The results show that the few-layer $ReSe_2$ SA sample exhibits

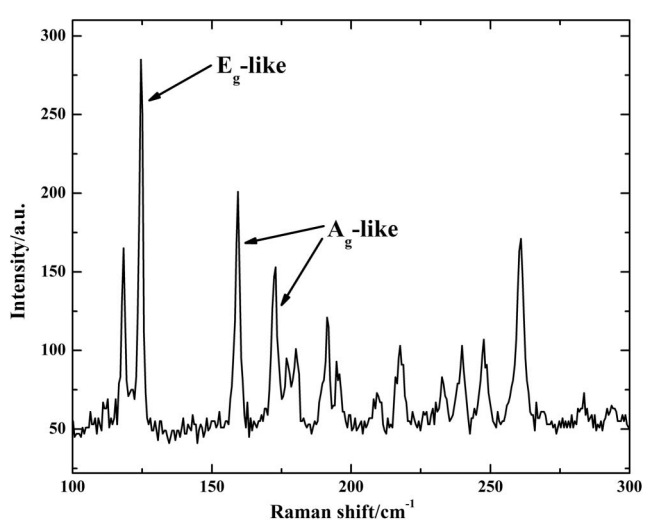

Fig. 1. Raman spectrum of $ReSe_2$ powder.

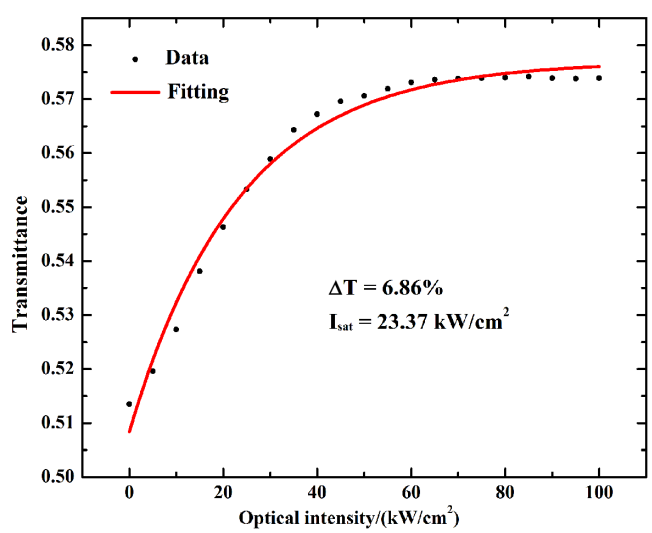

Fig. 3. Saturable absorption characteristic curve of $ReSe_2$ SA.

saturable absorption characteristics at 1.9 μm. The modulation depth was 6.86%, and the saturation intensity was 23.37 kW/cm^2. Compared with other SAs, experiments reported that WS_2 and $MoTe_2$ (one type of TMDs) both had a modulation depth of 6% near 2 μm and were successfully applied to all-solid-state passively Q-switched lasers[37,38]. Therefore, the $ReSe_2$ SA had a suitable modulation depth for a Tm:YLF laser experiment.

As shown in Fig. 4, a short concave-plane resonator was employed for the Tm:YLF Q-switched experiment. The resonator consisted of an input mirror M1 and an output mirror M2. The input mirror M1 was dichroic and had a curvature of 100 mm. The output mirror M2 had a transmission of 4%. To the rear of M1, the Tm:YLF crystal (3 mm × 3 mm × 10 mm, doped concentration of 3%) worked as the laser gain medium. It was wrapped with indium foil and cooled by water, whose temperature was stabilized at 18°C. Tm:YLF was pumped by a fiber-coupled diode laser (wavelength of 793 nm and core diameter of 400 μm). For the Q-switching laser, the $ReSe_2$ SA was placed close to M2, and the position and angle were carefully adjusted.

Figure 5 shows the average output power characteristics of the Tm:YLF laser. Under an absorbed pump power of 2.71 W, the Q-switched laser acquired the maximum average output power of 180 mW and a slope efficiency of 14.6%. At this power scope, the $ReSe_2$ SA was not observed with obvious damage. Power was measured by using a power meter [30(150)A-BB-18, Ophir].

A high-speed photodiode (PDA10PT-EC, Thorlabs) and a digital oscilloscope (MD03104, Tektronix) were used to measure the performance of the Q-switched pulses. When the absorbed pump power was added from 1.63 to 2.71 W, the pulse width and repetition rate were recorded, as shown in Fig. 6. In the experiment, the minimum pulse width of 1.61 μs at a repetition rate of 28.78 kHz was successfully generated. The corresponding pulse profiles are exhibited in Fig. 7. With $ReSe_2$ SA action, the profiles show a Q-switched pulse shape and a pulse train, respectively. With the shortest pulse width of 1.61 μs and the highest repetition rate of 28.78 kHz, the pulse energy and the peak power were calculated to be 6.25 μJ and 3.88 W.

Figure 8 shows the spectral characteristics measured by an optical spectrum analyzer (Mozza, Fastlite). The central wavelength of the Q-switched laser was 1906.5 nm.

In brief, $ReSe_2$ as an SA has been first, to the best of our knowledge, adopted to an all-solid-state passively Q-switched Tm:YLF laser. A $ReSe_2$ nanosheet was prepared by an ultrasonic stripping method. Its modulation depth was 6.86% at the wavelength of 1.9 μm. Under an absorbed pump power of 2.71 W, the Q-switched laser obtained a wavelength of 1906.5 nm, whose pulse width and repetition rate were 1.61 μs and 28.78 kHz, respectively. The maximum average output power was 180 mW, the pulse energy was 6.25 μJ, and the peak power was 3.88 W. Our experiment results proved that $ReSe_2$ possessed the saturable absorption property and could be used as an option for a near 2 μm SA. In the future,

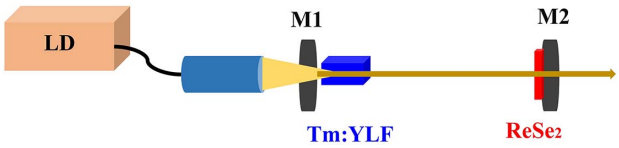

Fig. 4. Schematic diagram of laser cavity.

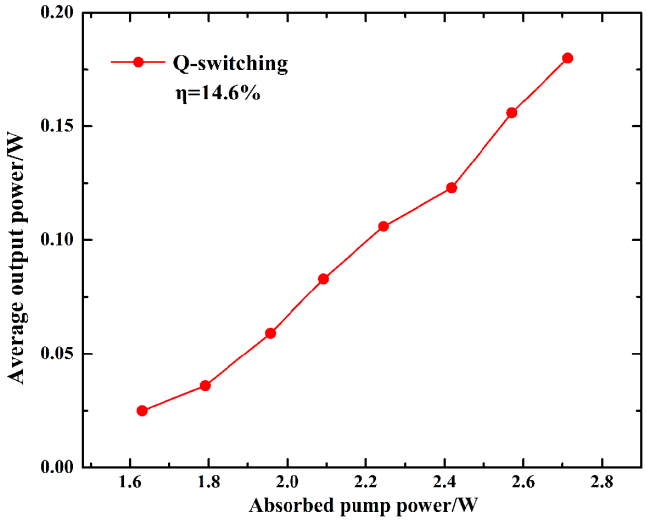

Fig. 5. Average output power versus absorbed pump power of the Q-switched laser.

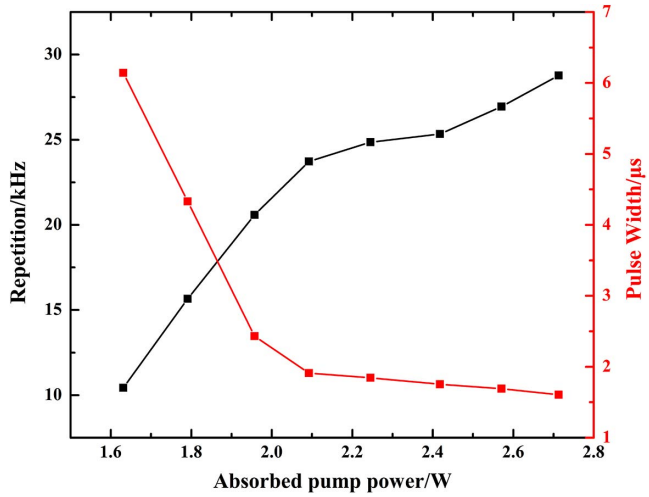

Fig. 6. Pulse width and repetition rate as functions of absorbed pump power.

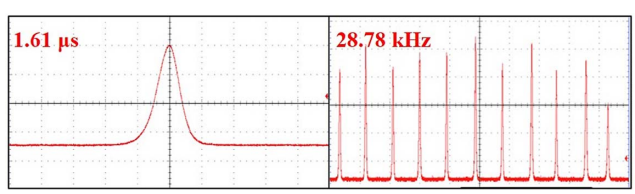

Fig. 7. Typical pulse profile of the Q-switched laser.

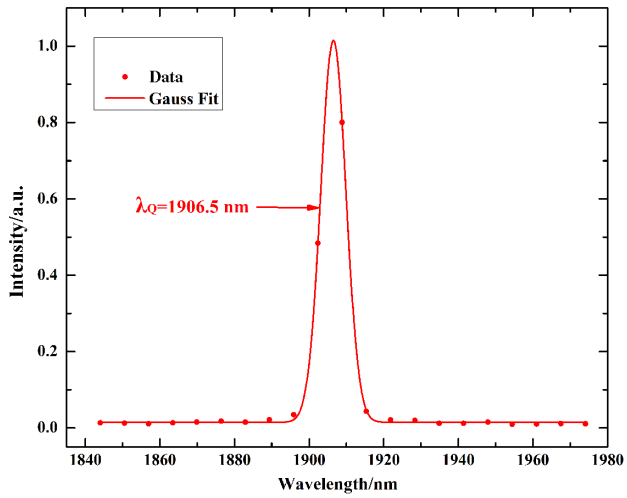

Fig. 8. Spectrum for Q-switching modes.

we will be devoted to optimizing the preparation of the $ReSe_2$ SA and the experimental design to obtain results with shorter pulse and excellent stability.

This work was supported by the Strategic Priority Research Program of the Chinese Academy of Sciences (No. XDB1603), the International S&T Cooperation Program of China (No. 2016YFE0119300), and the National Natural Science Foundation of China (NSFC) (Nos. 61521093 and 61505234).

References

1. W. Schmidt and F. P. Schäfer, Phys. Lett. A **26**, 558 (1968).
2. U. Keller, K. J. Weingarten, F. X. Kartner, D. Kopf, B. Braun, I. D. Jung, R. Fluck, C. Honninger, N. Matuschek, and J. A. Au, IEEE J. Sel. Top. Quantum Electron. **2**, 435 (1996).
3. S. Y. Set, H. Yaguchi, Y. Tanaka, and M. Jablonski, J. Lightwave Technol. **22**, 51 (2004).
4. D. D. Wu, H. Y. Lin, Z. P. Cai, J. Peng, Y. J. Cheng, J. Weng, and H. Y. Xu, IEEE Photon. J. **8**, 4501507 (2016).
5. H. D. Xia, H. P. Li, C. Y. Lan, C. Li, J. B. Du, S. J. Zhang, and Y. Liu, Photon. Res. **3**, A92 (2015).
6. H. Zhang, Q. L. Bao, D. Y. Tang, L. M. Zhao, and K. P. Loh, Appl. Phys. Lett. **95**, 141103 (2009).
7. Q. L. Bao, H. Zhang, Y. Wang, Z. H. Ni, Y. L. Yan, Z. X. Shen, K. P. Loh, and D. Y. Tang, Adv. Funct. Mater. **19**, 3077 (2009).
8. H. Zhang, D. Y. Tang, L. M. Zhao, Q. L. Bao, and K. P. Loh, Opt. Express **17**, 17630 (2009).
9. M. Breusing, C. Ropers, and T. Elsaesser, Phys. Rev. Lett. **102**, 086809 (2009).
10. D. D. Wu, Z. Q. Luo, F. Q. Xiong, C. K. Zhang, Y. Z. Huang, S. S. Chen, W. W. Cai, Z. P. Cai, and H. Y. Xu, IEEE Photon. Tech. Lett. **26**, 1474 (2014).
11. F. A. Rasmussen and K. S. Thygesen, J. Phys. Chem. C **119**, 13169 (2015).
12. Y. M. Shi, H. N. Li, and L. Li, Chem. Soc. Rev. **44**, 2744 (2015).
13. K. P. Wang, J. Wang, J. T. Fan, M. Lotya, A. O'Neill, D. Fox, Y. Y. Feng, X. Y. Zhang, B. X. Jiang, Q. Z. Zhao, H. Z. Zhang, J. N. Coleman, L. Zhang, and W. J. Blau, ACS Nano **7**, 9260 (2013).
14. H. Zhang, S. B. Lu, J. Zheng, J. Du, S. C. Wen, D. Y. Tang, and K. P. Loh, Opt. Express **22**, 7249 (2014).
15. H. Liu, A. P. Luo, F. Z. Wang, R. Tang, M. Liu, Z. C. Luo, W. C. Xu, C. J. Zhao, and H. Zhang, Opt. Lett. **39**, 4591 (2014).
16. R. Khazaeizhad, S. H. Kassani, H. Jeong, D. Yeom, and K. Oh, Opt. Express **22**, 23732 (2014).
17. B. Xu, Y. J. Cheng, Y. Wang, Y. Z. Huang, J. Peng, Z. Q. Luo, H. Y. Xu, Z. P. Cai, J. Weng, and R. Moncorgé, Opt. Express **22**, 28934 (2014).
18. J. Lu, X. Zou, C. Li, W. K. Li, Z. Z. Liu, Y. Q. Liu, and Y. X. Leng, Chin. Opt. Lett. **15**, 041401 (2017).
19. Z. C. Tiu, H. Ahmad, A. Zarei, and S. W. Harun, Chin. Opt. Lett. **14**, 041901 (2016).
20. W. J. Liu, L. H. Pang, H. N. Han, Z. W. Shen, M. Lei, H. Teng, and Z. Y. Wei, Photon. Res. **4**, 111 (2016).
21. Y. X. Sun, Y. Bai, D. Li, L. Hou, B. Bai, Y. Z. Gong, L. L. Yu, and J. T. Bai, Opt. Express **25**, 21037 (2017).
22. Z. Q. Luo, D. D. Wu, B. Xu, H. Y. Xu, Z. P. Cai, J. Peng, J. Weng, S. Xu, C. H. Zhu, F. Q. Wang, Z. P. Sun, and H. Zhang, Nanoscale **8**, 1066 (2016).
23. D. D. Wu, Z. R. Guo, J. Peng, J. Weng, Z. P. Cai, and H. Y. Xu, Appl. Opt. **57**, 4955 (2018).
24. R. T. Lv, J. A. Robinson, R. E. Schaak, D. Sun, Y. F. Sun, T. E. Mallouk, and M. Terrones, Acc. Chem. Res. **48**, 56 (2015).
25. C. H. Ho, Y. S. Huang, K. K. Tiong, and P. C. Liao, Phys. Rev. B **58**, 16130 (1998).
26. H. X. Zhong, S. Y. Gao, J. J. Shi, and L. Yang, Phys. Rev. B **92**, 115438 (2015).
27. M. Hafeez, L. Gan, H. Q. Li, Y. Ma, and T. Y. Zhai, Adv. Mater. **28**, 8296 (2016).
28. E. Z. Zhang, P. Wang, Z. Li, H. F. Wang, C. Y. Song, C. Huang, Z. G. Chen, L. Yang, K. T. Zhang, S. H. Lu, W. Y. Wang, S. S. Liu, H. H. Fang, X. H. Zhou, H. G. Yan, J. Zou, X. G. Wan, P. Zhou, W. D. Hu, and F. X. Xiu, ACS Nano **10**, 8067 (2016).
29. D. Wolverson, S. Crampin, A. S. Kazemi, A. Ilie, and S. J. Bending, ACS Nano **8**, 11154 (2014).
30. F. F. Cui, X. B. Li, Q. L. Feng, J. B. Yin, L. Zhou, D. Y. Liu, K. Q. Liu, X. X. He, X. Liang, S. Z. Liu, Z. B. Lei, Z. H. Liu, H. L. Peng, J. Zhang, J. Kong, and H. Xu, Nano Res. **10**, 2732 (2017).
31. F. Qi, X. Q. Wang, B. J. Zheng, Y. F. Chen, B. Yu, J. H. Zhou, J. R. He, P. J. Li, W. L. Zhang, and Y. R. Li, Electrochim. Acta **224**, 593 (2017).
32. S. X. Yang, C. Wang, H. Sahin, H. Chen, Y. Li, S. S. Li, A. Suslu, F. M. Peeters, Q. Liu, J. Li, and S. Tongay, Nano Lett. **15**, 1660 (2015).
33. C. H. Ho, P. C. Liao, Y. S. Huang, T. R. Yang, and K. K. Tiong, J. Appl. Phys. **81**, 6380 (1997).
34. L. Du, G. B. Jiang, L. L. Miao, B. Huang, J. Yi, C. J. Zhao, and S. C. Wen, Opt. Mater. Express **8**, 926 (2018).
35. K. D. Niu, Q. Y. Chen, R. Y. Sun, B. Y. Man, and H. N. Zhang, Opt. Mater. Express **7**, 3934 (2017).
36. Y. Chen, C. J. Zhao, H. H. Huang, S. Q. Chen, P. H. Tang, Z. T. Wang, S. B. Lu, H. Zhang, S. C. Wen, and D. Y. Tang, J. Lightwave Technol. **31**, 2857 (2013).
37. C. Luan, K. J. Yang, J. Zhao, S. Z. Zhao, L. Song, T. Li, H. W. Chu, J. P. Qiao, C. Wang, Z. Li, S. Z. Jiang, B. Y. Man, and L. H. Zheng, Opt. Lett. **41**, 3783 (2016).
38. B. Z. Yan, B. T. Zhang, H. K. Nie, H. Y. Wang, G. R. Li, X. L. Sun, R. H. Wang, N. Lin, and J. L. He, Opt. Express **26**, 18505 (2018).